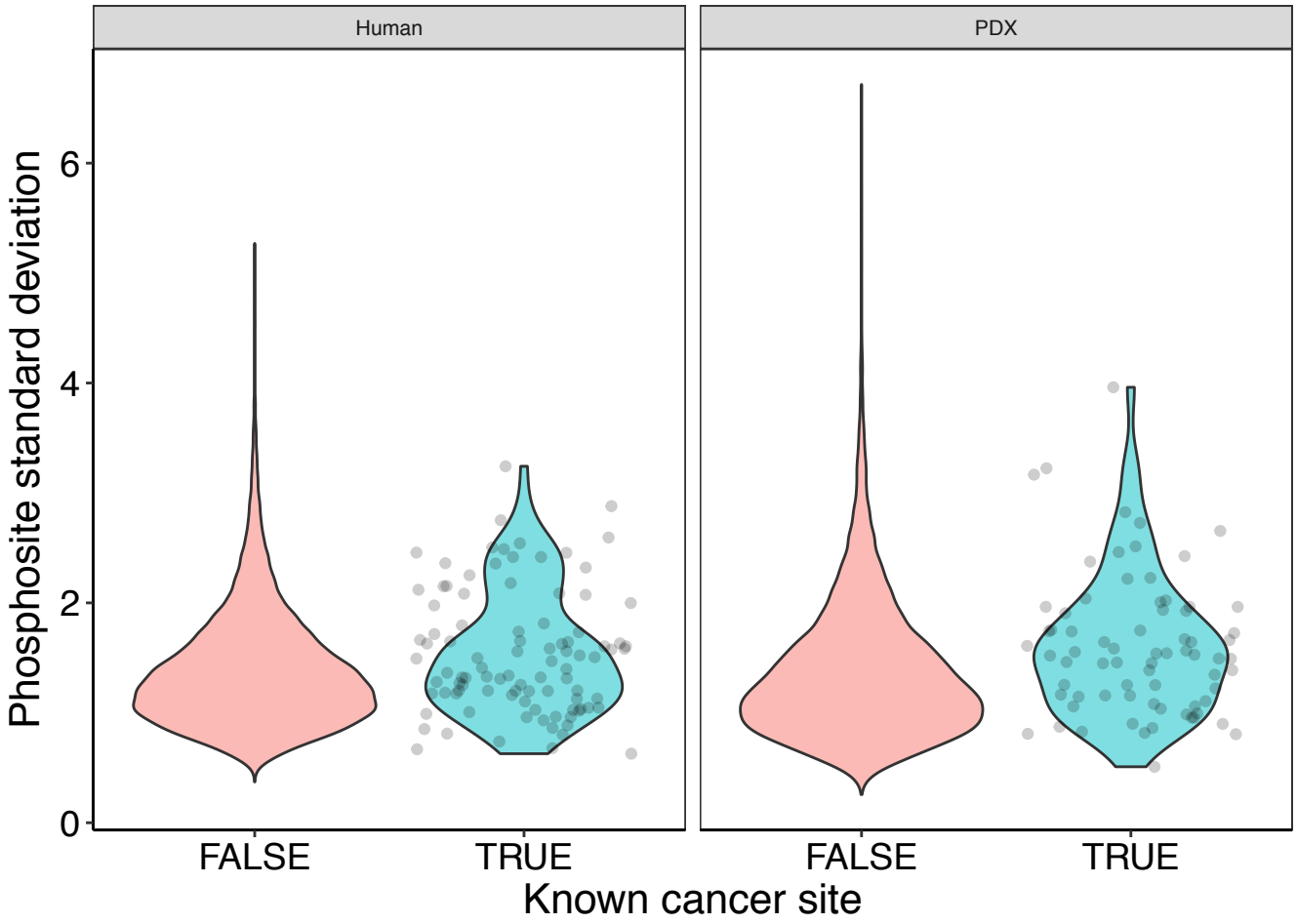

Supplementary Figure 1. Comparison of standard deviation of known cancer-related phosphosites vs. other phosphosites in human and PDX breast cancer samples.

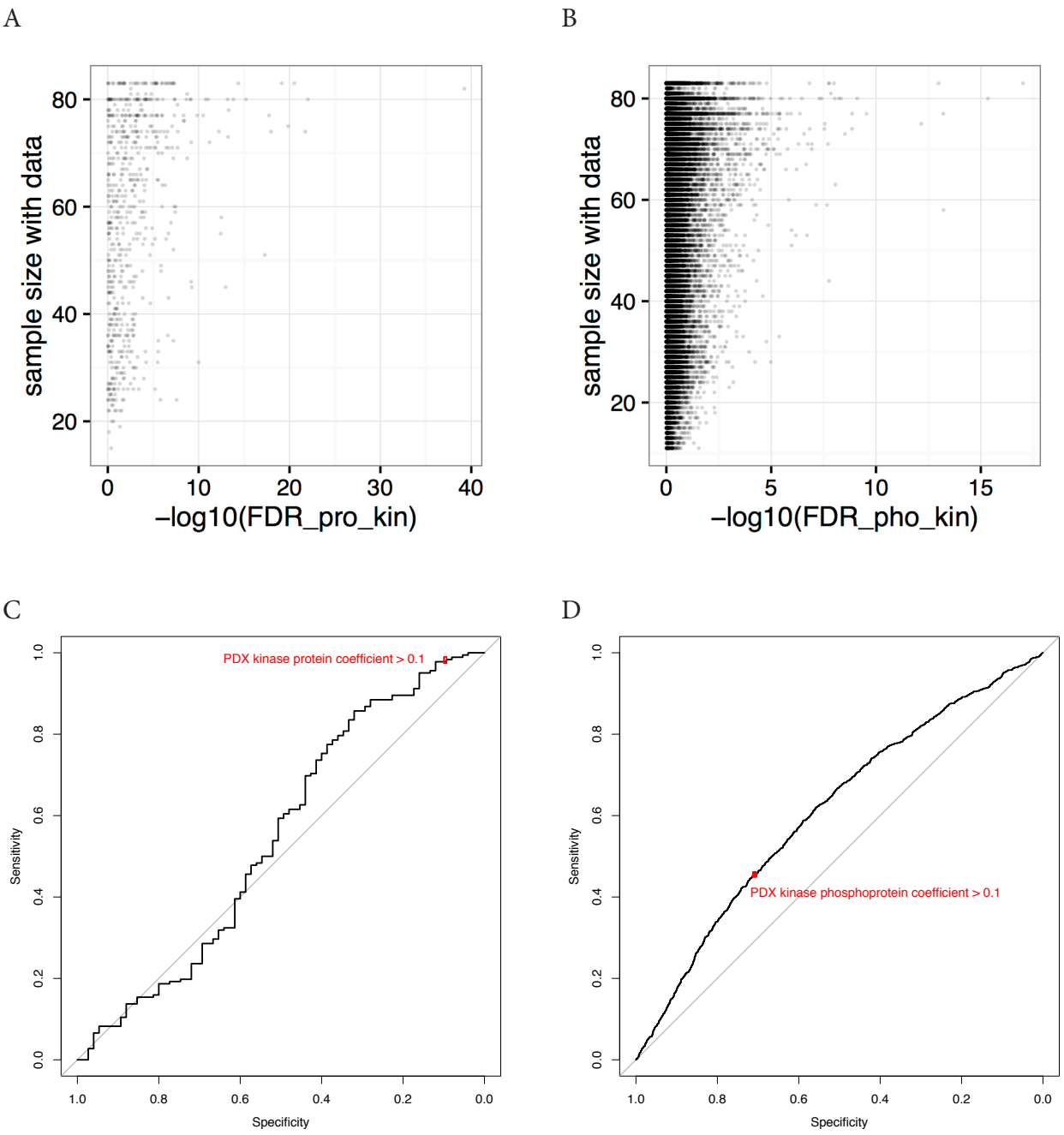

Supplementary Figure 2. Cis/trans pair discovery and validation. Relationship between observed sample size and significance of kinase-substrate coefficient in (A) cis and (B) trans analyses. Volcano plot showing threshold used for validation in the (C) cis and the (D) trans analyses using the PDX cohort.

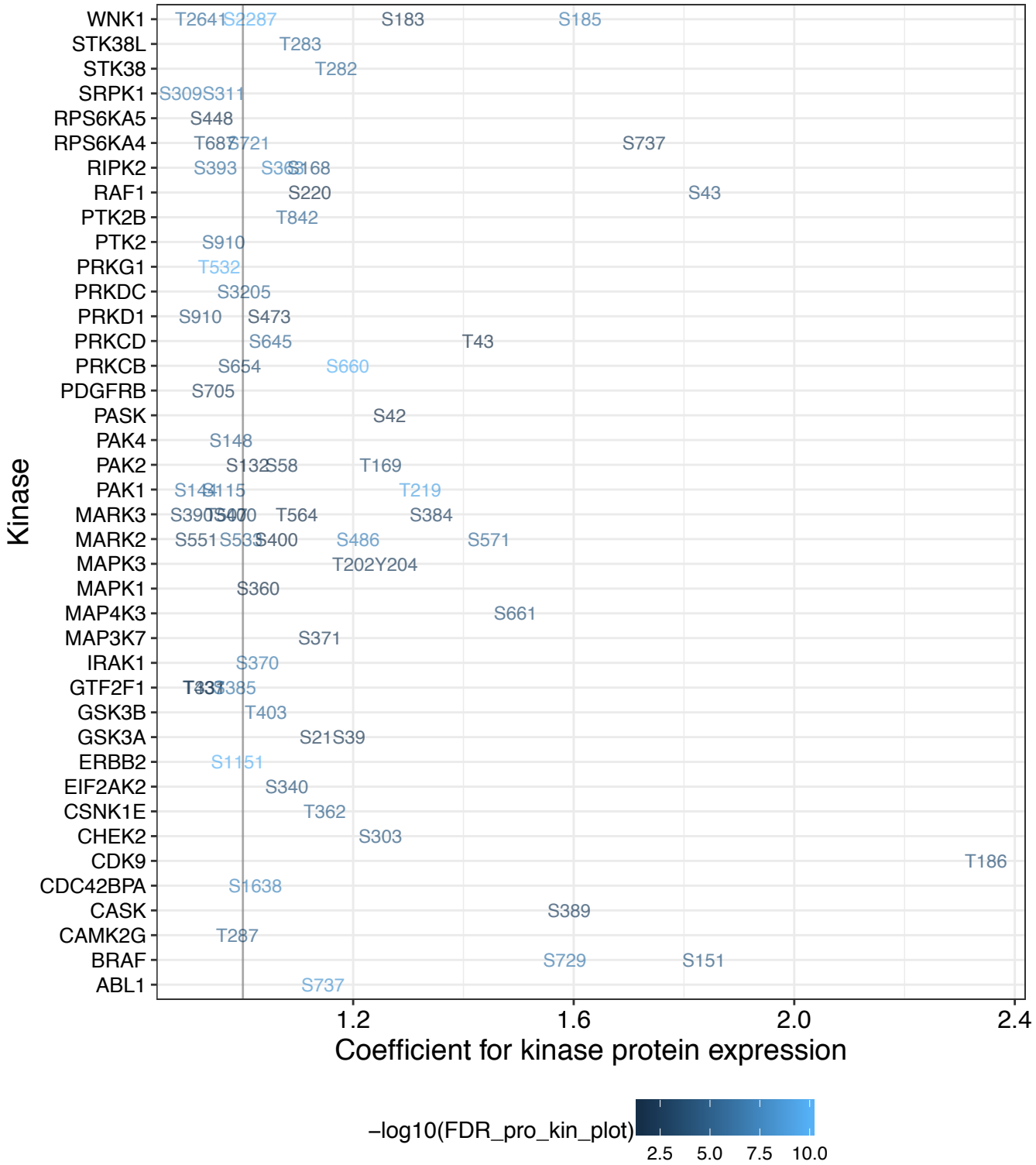

Supplementary Figure 3. Potentially auto-phosphorylated cis kinase-phosphosite pairs in breast cancer with regression coefficient equal to or greater than 1.

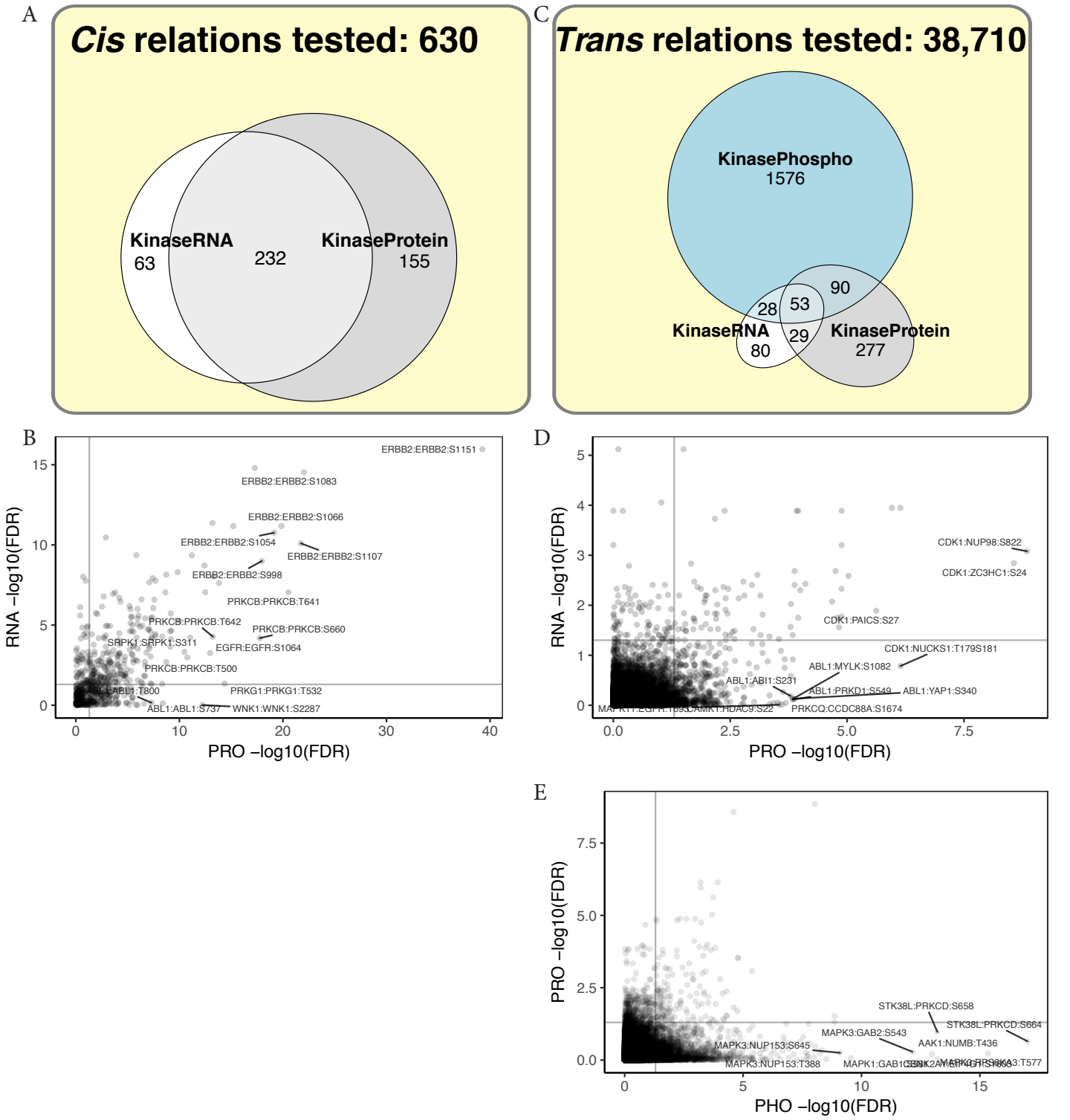

Supplementary Figure 4. Regulation of kinase-substrate pairs identified using various models. (A) Venn diagrams showing the numbers of cis-regulated phosphosites identified through quantitative association using kinase RNA or protein levels as the independent variable. (B) Comparison of significance level (-log10FDR) of cis-regulated pairs obtained through using the kinase-RNA and kinase-protein models. (C) Venn diagrams showing the numbers of trans-regulated phosphosites identified through quantitative association using kinase RNA, protein or phosphoprotein level as the independent variable. (D) Comparison of significance level (-log10FDR) of trans-regulated pairs obtained through using the kinase-RNA and kinase-Protein models. (E) Comparison of significance level (-log10FDR) of trans-regulated pairs obtained through using the kinase-protein and kinase-phosphoprotein models.

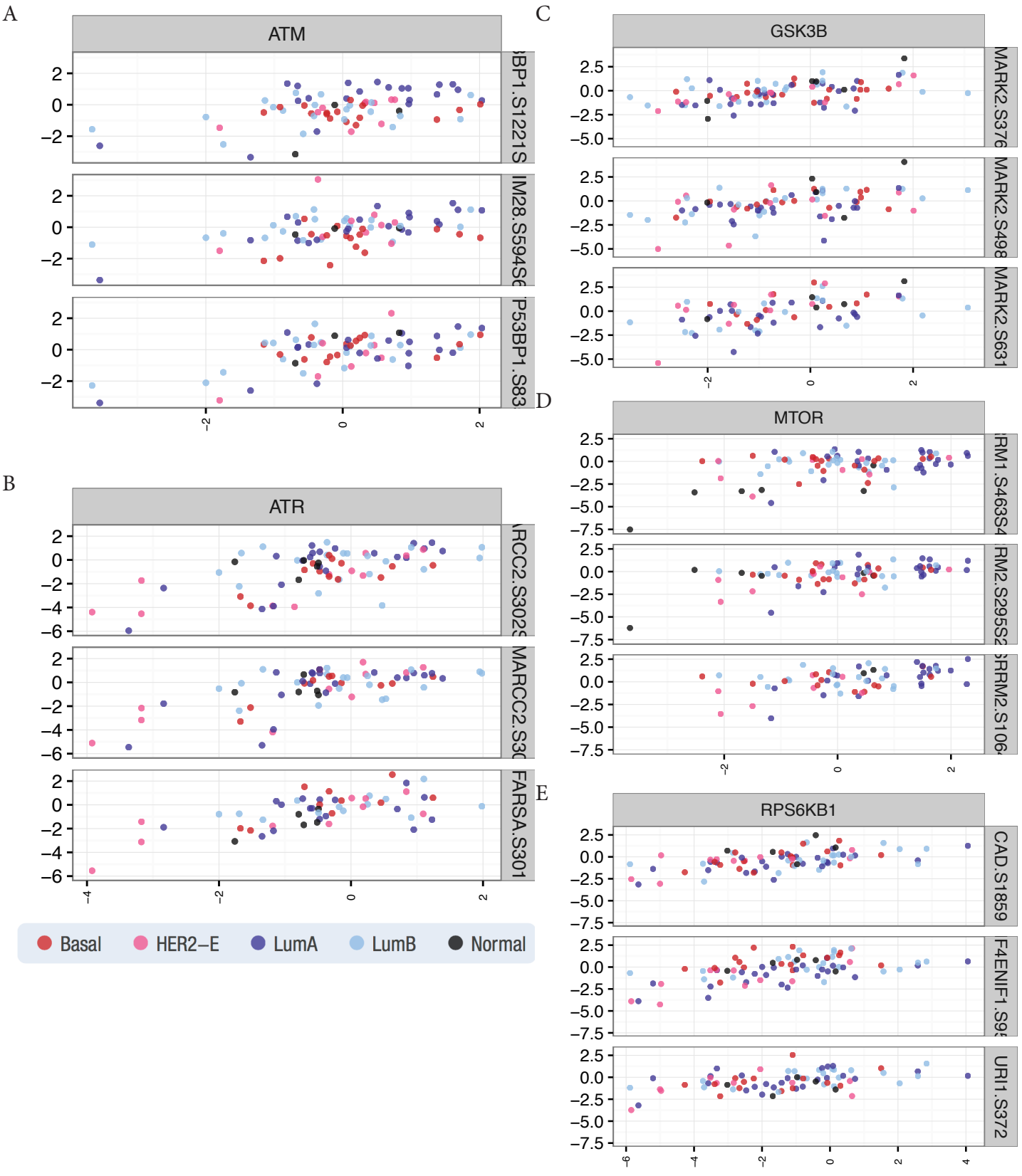

Supplementary Figure 5. Top trans-regulated phosphosites of (A) ATM (B) ATR, (C) GSK3B, (D) MTOR, and (E) RPS6KB1.

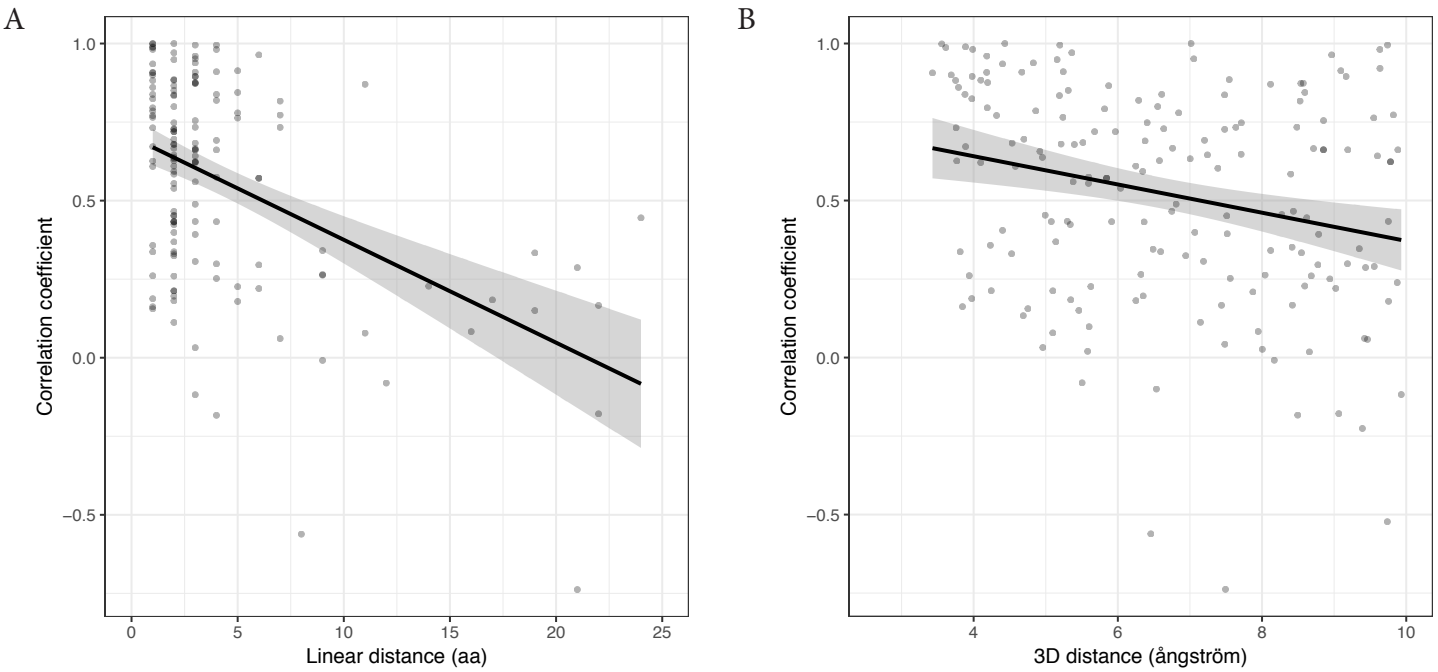

Supplementary Figure 6. Correlation between (A) linear and (B) 3D distances and correlations of phosphosite pairs on the same PDB structure.

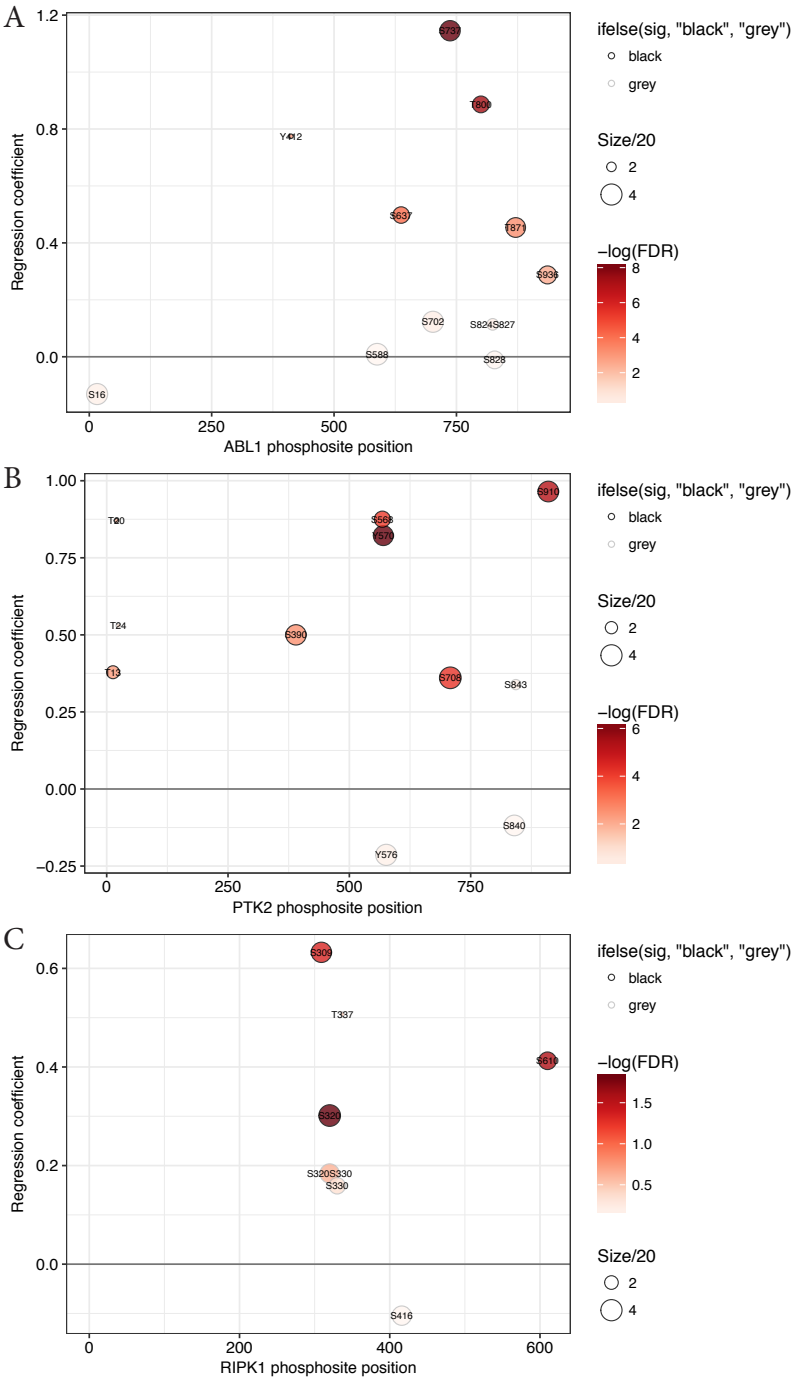

Supplementary Figure 7. Landscape of cis-regulation of phosphosites in (A) ABL1 (B) PTK2 and (C) RIPK1.

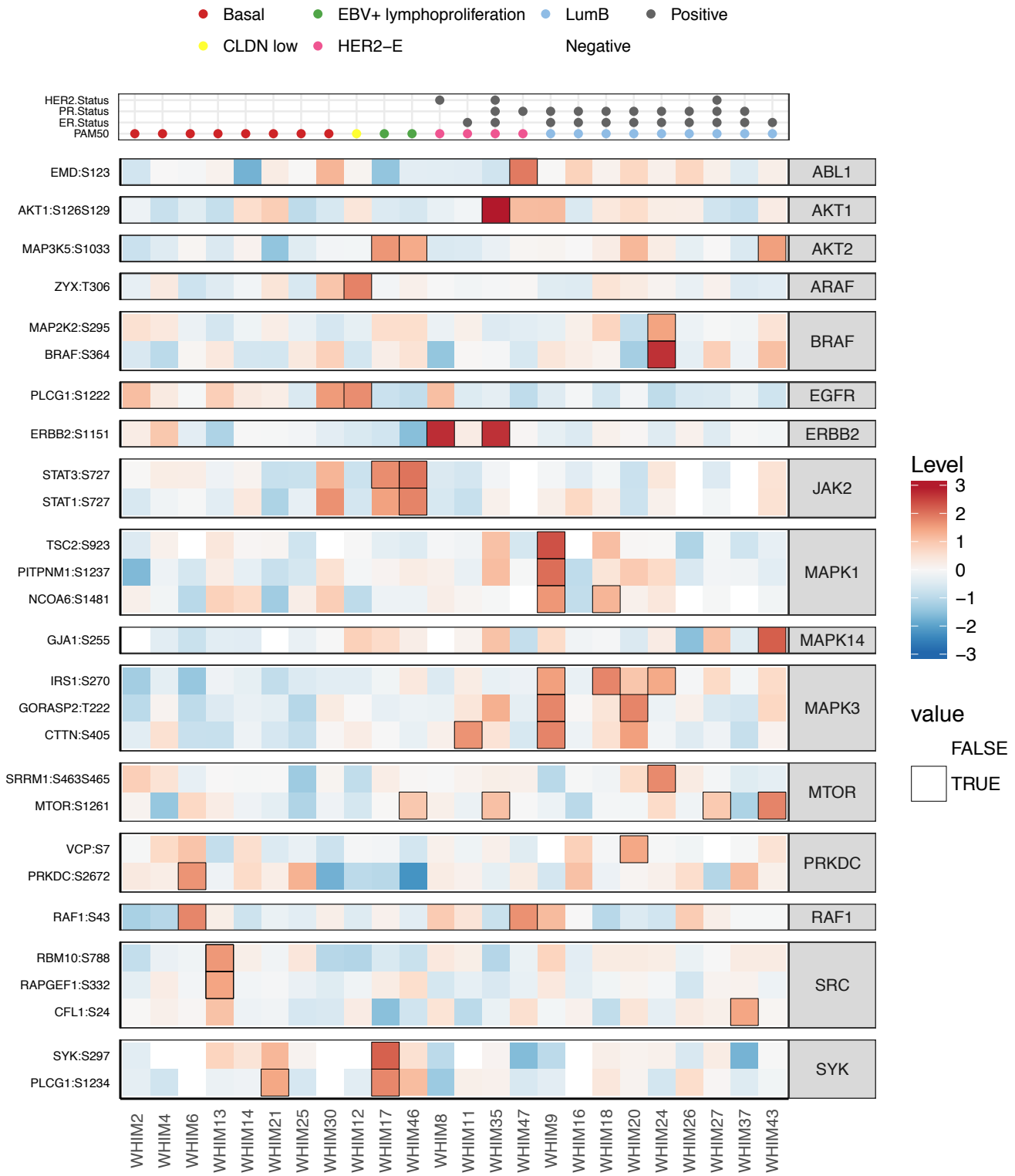

Supplementary Figure 8. Heatmap of regulated kinase-substrate pairs where the kinase or the substrate is a potential druggable target in 24 breast cancer PDX. The sample-pair showing outlier pair event is outlined. Only the top 3 regulated pairs were shown for each kinase when there were more than 3 pairs showing kinase-substrate outliers.

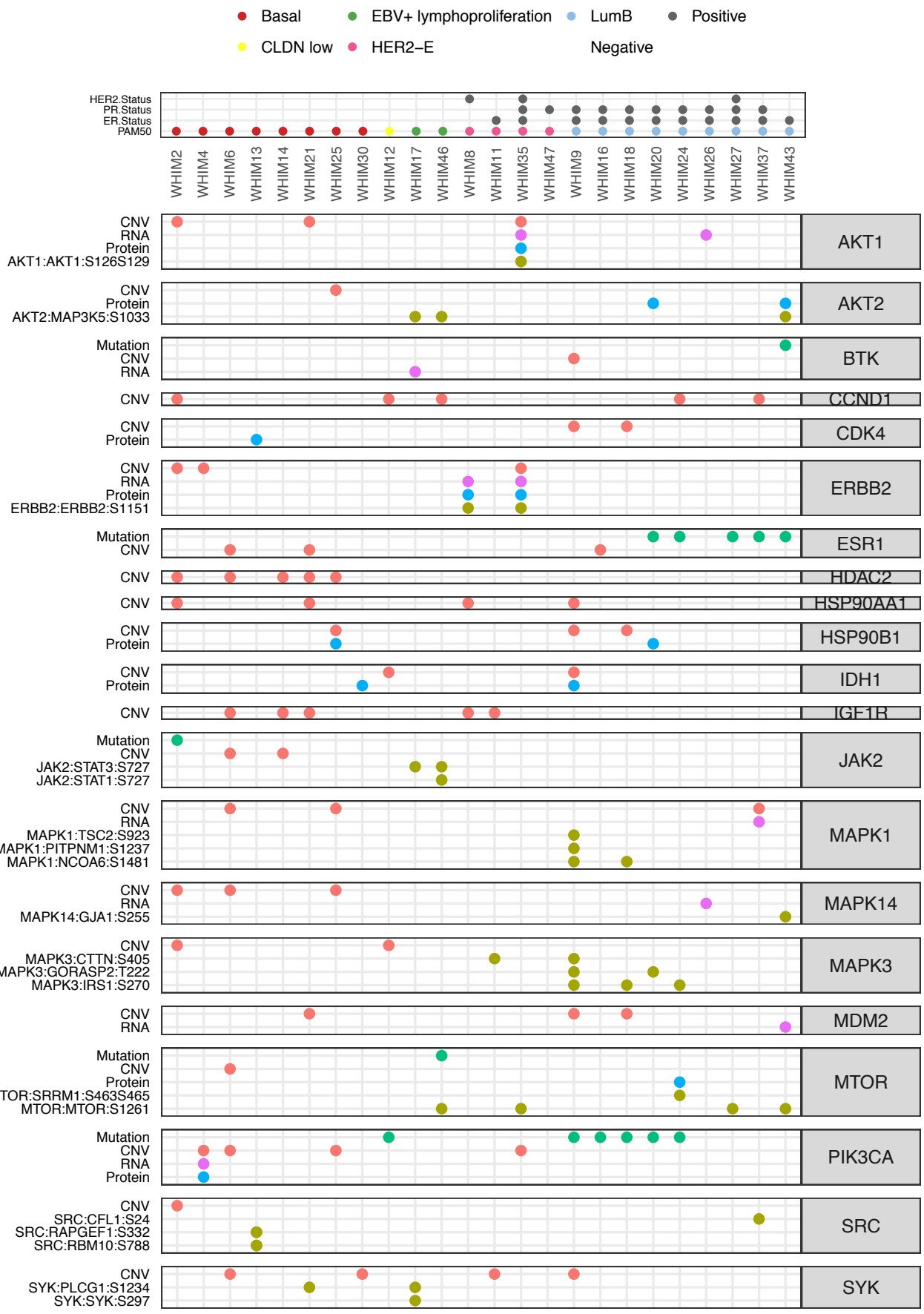

Supplementary Figure 9. Druggability analysis of single and paired events in 24 breast cancer PDX samples. Druggable events identified in the mutation, CNV, RNA, protein and phospho-pair level for breast cancer PDX samples.

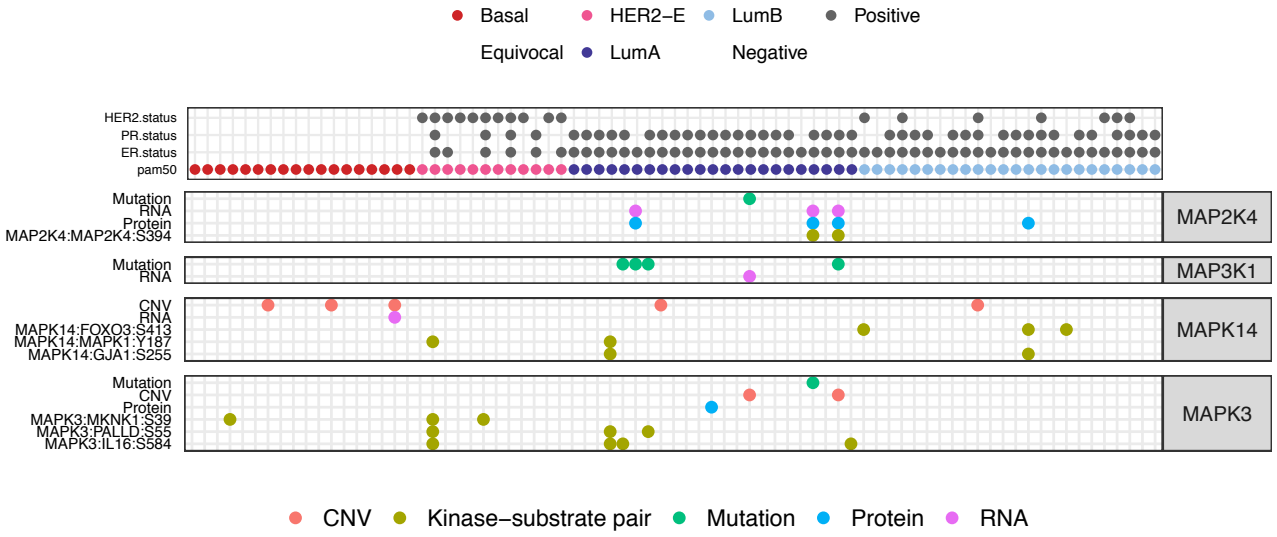

Supplementary Figure 10. Druggable events identified in the mutation, CNV, RNA, protein and phospho-pair level showing members of the MAP kinase cascades.

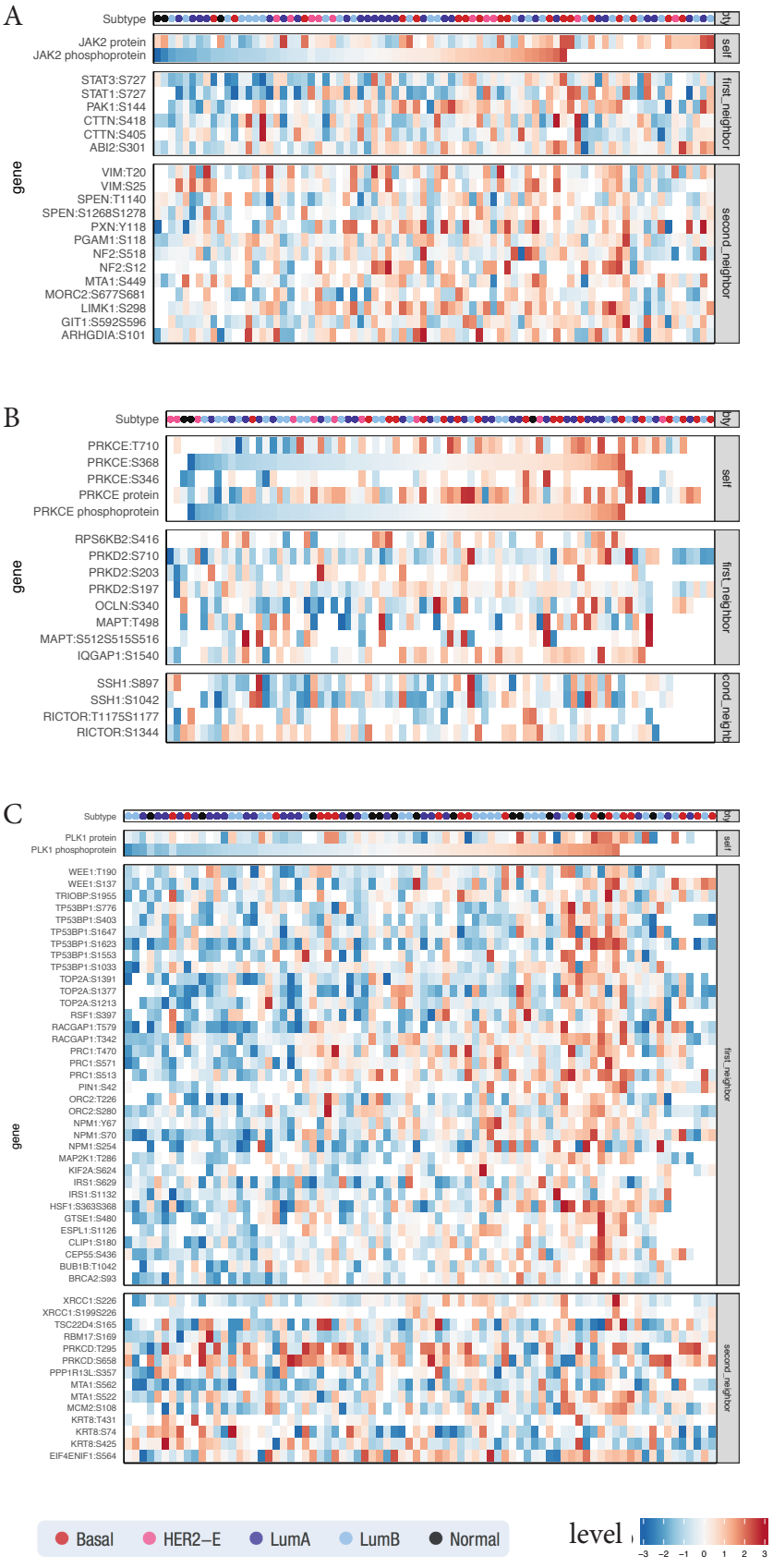

Supplementary Figure 11. Druggable kinase-substrate cascades originating from (A) JAK2 (B) PRKCE and (C) PLK1 in the 77 breast cancer samples. The samples in the heatmap were ordered by the phosphoprotein level of each of the kinase.

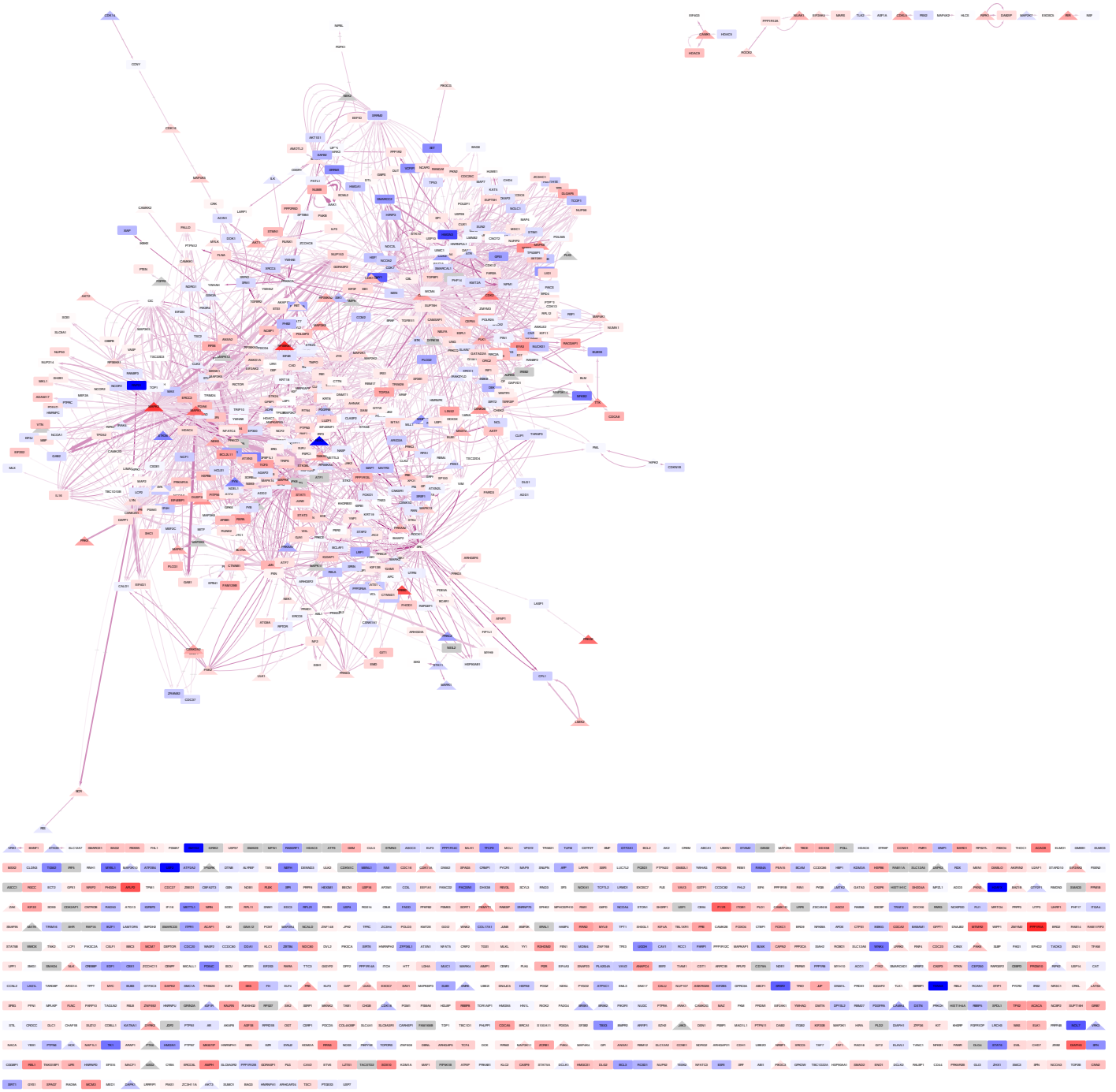

Supplementary Figure 12. Landscape of cis and trans-regulations identified in the breast cancer cohort. For each node of the network diagrams, the color represents the relative level of basal compared to luminal A/B breast cancers, where blue indicates higher level in luminal and red indicates higher level in basal tumors. For the edges, the darkness of the color is scaled by the degree of correlation coefficient and the width is scaled by -log(FDR) of the association.

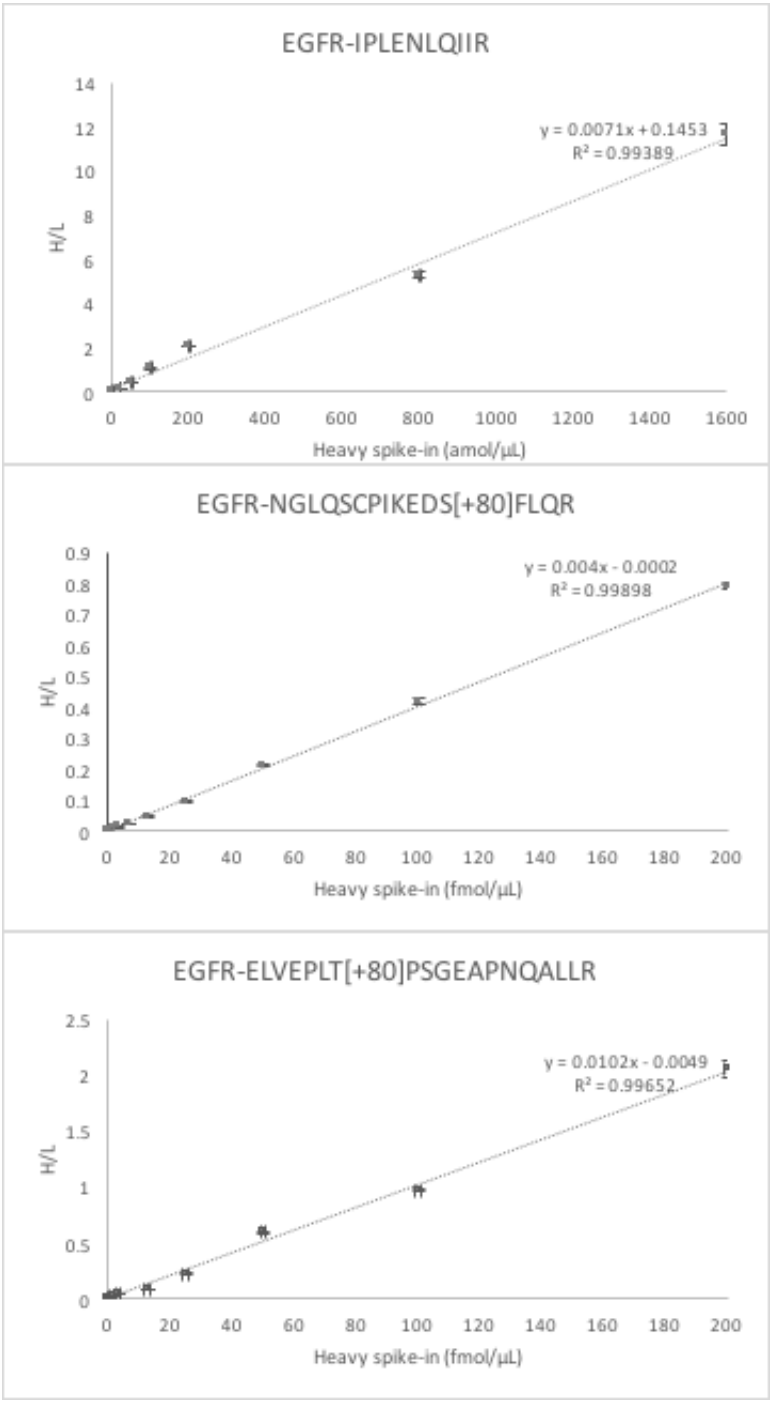

Supplementary Figure 13. Response curves for three EGFR peptides. For peptide IPLENLQIIR, varying concentrations of heavy peptide (0, 20, 50, 100, 200, 800 and 1600 amol/μL) and a constant concentration of light peptide (125 amol/μL) were spiked into a tryptic digest of a human breast cancer xenograft tissue (0.1 μg peptide) and 5 μL of sample at each data point was analyzed by LC-SRM. Its limit of detection (LOD) and lower limit of quantification (LLOQ) were both determined at 20 amol/μL level. For the two phosphopeptides NGLQSCPIKED(pS)FLQR and ELVEPL(pT)PSGEAPNQALLR, varying concentrations of heavy peptide (0, 0.4, 0.8, 1.6, 3.125, 6.25, 12.5, 25, 50, 100, and 200 fmol/μL) and a constant concentration of light peptide (200 fmol/μL) were spiked into the same breast tumor xenograft sample (100 μg peptide), followed by IMAC enrichment of the phosphopeptides and LC-SRM analysis. The LOD and LLOQ for both phosphopeptides were 0.4 fmol/μL and 1.6 fmol/μL, respectively. The LOD was determined by S/N>3, and the LLOQ was determined by both S/N>10 and CV<20%.

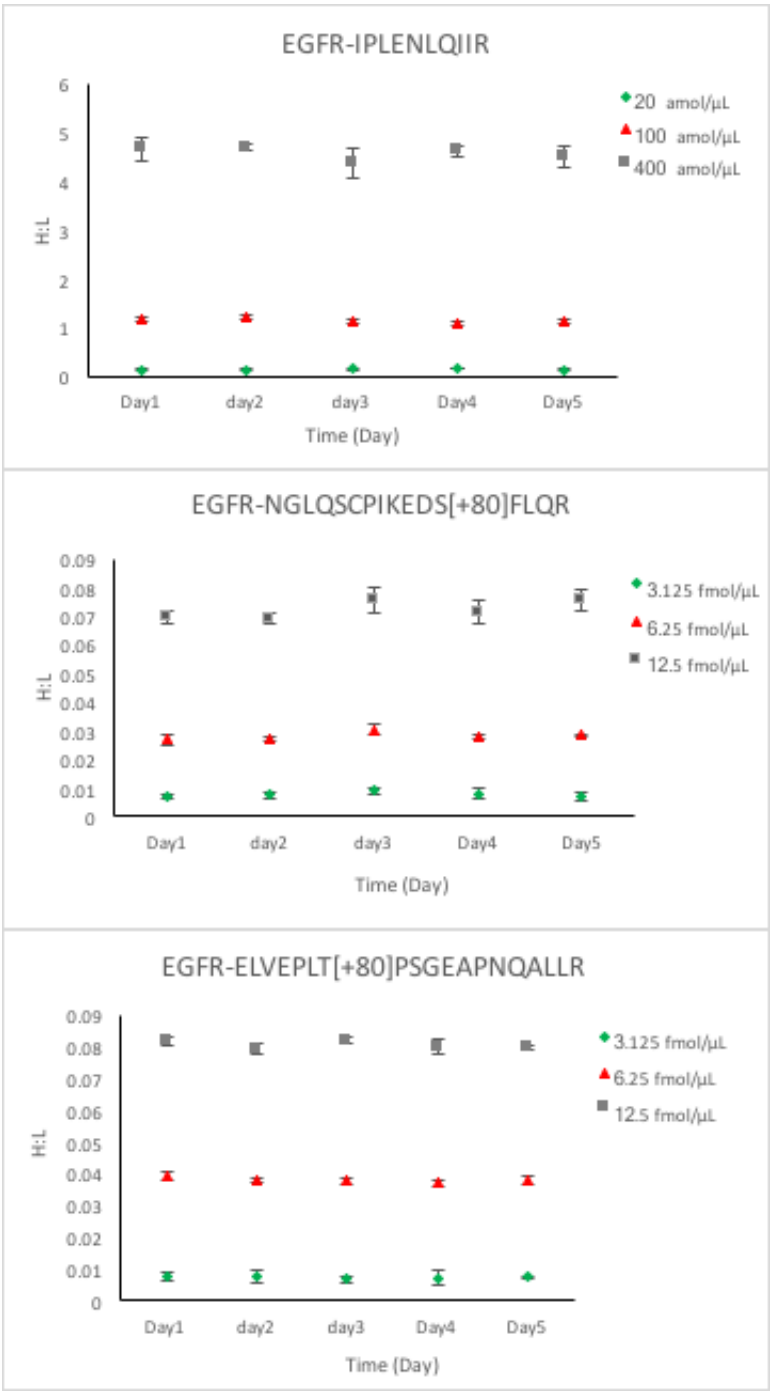

Supplementary Figure 14. Inter-day experiment for three EGFR peptides. For peptide IPLENLQIIR, 20, 100 and 400 amol/µL concentrations and a constant amount of light peptide (125 amol/µL) were spiked into a tryptic digest of a human breast cancer xenograft tissue (0.1 µg peptide) and 5 µL of sample at each data point was analyzed by LC-SRM. The inter-day CVs for all three measured concentrations ranged from 1.4% to 14%. For the two phosphopeptides NGLQSCPIKED(pS)FLQR and ELVEPL(pT)PSGEAPNQALLR, 3.125, 6.25 and 12.5 fmol/µL and a constant amount of light peptide (200 fmol/µL) were spiked into the same breast tumor xenograft sample (100 µg peptide), followed by IMAC enrichment of the phosphopeptides and LC-SRM analysis. The inter-day CVs for all three measured concentrations ranged from 1.2% to 24% and 0.5% to 13% for NGLQSCPIKED(pS)FLQR and ELVEPL(pT)PSGEAPNQALLR, respectively.